

CHAPTER 1

BLOCK COPOLYMER THIN FILMS

Jia-Yu Wang, Soojin Park, Thomas P. Russell
Department of Polymer Science and Engineering
University of Massachusetts, Amherst
Amherst, MA 01003, U.S.A.
E-mail: russell@mail.pse.umass.edu

The behavior of amorphous block copolymers (BCPs) in thin films depends on a combination of segmental interactions, interfacial interactions, surface energies and entropy. Commensurability between the film thickness, h , and the natural period, L_0 , of the microdomains in the bulk is also of importance. This chapter summarizes recent developments in our understanding of the influence of confinement, surface energies and surface heterogeneities on the morphology of BCP thin films, the use of thin BCP films as scaffolds and templates for the fabrication of nanostructured materials, and the generation BCP arrays in thin films having long-range lateral order for potential addressable media.

1. Introduction

Block copolymers (BCPs) consist of two or more chemically different polymer chains joined covalently at their ends. Due to the positive enthalpy and small entropy of mixing, dissimilar blocks tend to microphase separate into well-ordered arrays of domains, classically termed microdomains. The sizes of these microdomains, due to the connectivity of the blocks, are limited to molecular dimensions and, as such, are tens of nanometers or less. At temperature below an order-to-disorder transition temperature, T_{ODT} , BCPs microphase separate into

arrays of spherical, cylindrical, gyroid or lamellar microdomains, depending on the volume fractions of the blocks, f , and the degree of microphase separation, χN , where χ is the Flory-Huggins segmental interaction parameter and N is the total number of segments in BCPs. Above the T_{ODT} , BCPs phase mix and are disordered.

The self-assembly of BCPs into well-defined morphologies has opened numerous applications ranging from drug delivery to structural materials. In contrast to the bulk, the morphology of amorphous BCP thin films can be strongly influenced by surface and interfacial energies as well as the commensurability between the film thickness, h , and the period of the microdomain morphology, L_0 . With decreasing film thickness these parameters become increasingly important in defining the morphology. By controlling the orientation and lateral ordering the BCP microdomains in thin films, unique opportunities in the use of BCPs in materials science (adhesive properties, lubrication, membranes, and coatings), lithography and microfabrication (addressable memory, magnetic storage, insulating foams) and device technologies (light-emitting diodes, photodiodes, and transistors) are beginning to emerge. In this chapter, two aspects of BCP thin films will be addressed. First, the effect of confinement, surface energies and surface heterogeneities on the morphology of BCP thin films will be discussed on the basis of the simplest and most studied system, namely thin films of compositionally symmetric, amorphous diblock copolymers. This is followed by a review of BCP thin films for nanopatterning with discussion centering on fabrication of long-range ordered nanostructures of BCP thin films by applying various external fields.

2. Morphologies of BCP Thin Films

2.1. *Effect of Confinement*

The presence of a surface or interface can strongly influence the phase behavior, morphology and kinetics of a multicomponent system. Understanding of the influence of boundary surfaces, in particular, commensurability and interfacial interactions, on the morphology of BCP thin films has attracted much attention. Phenomena like

symmetric/asymmetric wetting, surface topographies of “islands” or “holes”, surface-induced ordering, and commensurability have been extensively studied.

Symmetric/Asymmetric Wetting. Consider a thin film of a block copolymer below T_{ODT} . The connectivity of the block means that the film thickness is not arbitrary but rather defined in terms of L_0 .¹⁻¹⁹ For an A-*b*-B BCP, if A or B preferentially locates at both the surface and substrate interface, i.e. symmetric wetting, then the film thickness, h , is defined by nL_0 where n is an integer. If, on the other hand, different blocks segregate to the interfaces, then the film thickness is given by $(n+1/2)L_0$. So, to a first approximation, a thin BCP film is smooth, only if these constraints are satisfied. In all other cases, a surface topography consisting of islands or holes are seen where the step height is L_0 . Examples of these are shown in the scanning force micrographs in Figure 1. Optical microscopy can also be used where discrete interference colors are seen, corresponding to the different thickness or optical path lengths.

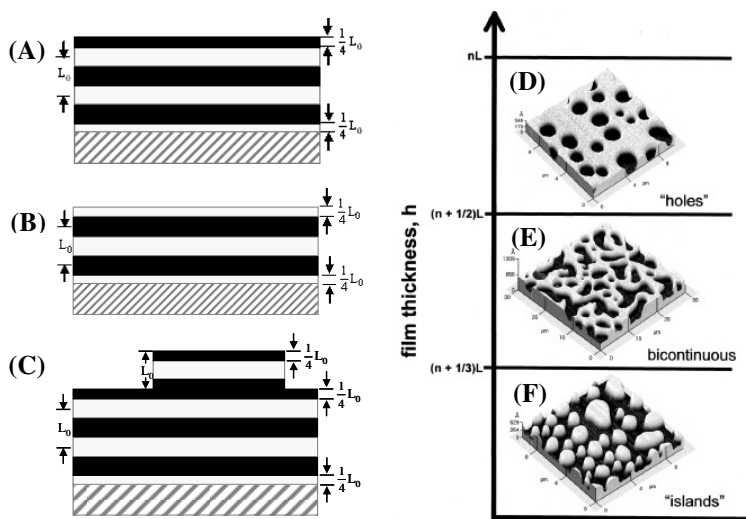


Fig. 1. (A-C) Schematic of three types of film structures. (A) $h = H_n = (n+1/2)L_0$; (B) $h = H_n = nL_0$; (C) $(h = H_n + \Delta h)$. (D-E) AFM images of topographical features of (D) holes; (E) bicontinuous and (F) islands. Reproduced with permission from *Advances in Colloid and Interface Science*.¹⁸

It should be noted that if h is not much different than nL_0 or $(n+1/2)L_0$ for symmetric or asymmetric wetting conditions, respectively, then a surface topography may not be seen and the copolymer chains can stretch or compress to accommodate this incommensurability. This, of course, depends on a balance of the energy associated with stretching or compressing the BCP chains and the additional energy arising from the generation of more surface areas.

Frustration. If the film is confined between two parallel, impenetrable walls, having strong interactions with either A or B block, a surface topography cannot form and the incommensurability between L_0 and h causes a frustration, since the hard boundaries prohibit the formation of surface topography and the characteristic period of BCPs must change to accommodate this frustration. Lambooy et al.^{19, 20} and, subsequently Koneripalli et al.⁶ developed techniques to suppress the formation of surface topography by confining copolymer thin films between two hard walls. Strong interactions of the blocks with the confining walls were sufficient to force the period of BCPs to expand or compress by as much as 50% in some cases. Kickuchi and Binder,^{21, 22} Turner²³ and Walton et al.⁹ theoretically examined the confinement of lamellar BCPs and found that the frustration imposed on BCPs chains by thickness constraints depended strongly on the strength of the interactions of the blocks with the substrate. In the case of strong interactions, stretched or compressed copolymer multilayers were predicted. However, as observed by Lambooy et al.,⁷ as the interactions of the copolymer with the confining walls became weaker, the copolymer domains can change their orientation with respect to the substrate, i.e. orient normal to the wall interface, allowing the period of the copolymer to be L_0 but paying the energetic price associated with unfavorable interaction at the interfaces.

Surface-Induced Instabilities. For $T > T_{ODT}$, if BCPs film is thinner than a characteristic thickness, i.e. $h < h_t$, ($h_t = L_0$ for symmetric wetting and $1/2L_0$ for asymmetric wetting), a “spinodal-like” pattern forms on the surface due to the frustration mentioned above. Prior to the formation of the surface topography, the film is unstable and shows periodic fluctuations.^{18, 24-27} These surface patterns form spontaneously across the

film surface, similar to a film undergoing dewetting. In the BCPs cases, though, the substrate is the initial copolymer layer that is preferentially located at the substrate. When $h = h_t$, the film is stable and the surface remains smooth. For films of $h > h_t$, a layer of thickness $h - h_t$ becomes unstable and dewets an underlying layer of thickness h_t , forming “islands”, “holes” or a “spinodal-like” topography. This type of autophobic dewetting has not been observed in homopolymers.^{18, 28-30}

Surface-Induced Ordering. The presence of a surface can induce ordering of a phase-mixed copolymer, i.e. when $T > T_{ODT}$.^{1, 7, 16, 26, 31-42} This was first predicted by Fredrickson using mean-field theoretical arguments.⁴² Anastasiadis et al. experimentally verified this prediction in a neutron reflectivity study on BCPs of polystyrene and poly(methyl methacrylate), denoted PS-*b*-PMMA. By fitting the scattering length density profiles, it was shown that the ordering decays exponentially from the surface with a correlation length very close to the bulk correlation length, in agreement with the arguments of Fredrickson.⁴² Subsequently, Menelle et al.³⁸ studied film thickness dependence of the ordering transition temperature and found that T_{ODT} was significantly elevated by the surface-induced ordering and, in fact, an order-to-disorder transition did not exist in thin films since the order parameter did not decay to zero at any point in the film. However, the films were shown to undergo a transition from a partially to a fully ordered state at a temperature that depended in a power-law manner on the film thickness, as shown in Figure 2.

2.2. Surface Energy

The morphology of BCP thin films is strongly influenced by the strength of interfacial interactions.⁴³⁻⁵⁶ Strong preferential interactions of one block with the substrate or a lower surface energy of one component causes a segregation of that block to either the surface of the film or the substrate interface. As a result, the connectivity of the blocks forces a parallel orientation of the microdomain to the substrate. When the surface is neutral, i.e., the interfacial interactions of both blocks are equally favorable or unfavorable, there is no preferential segregation of

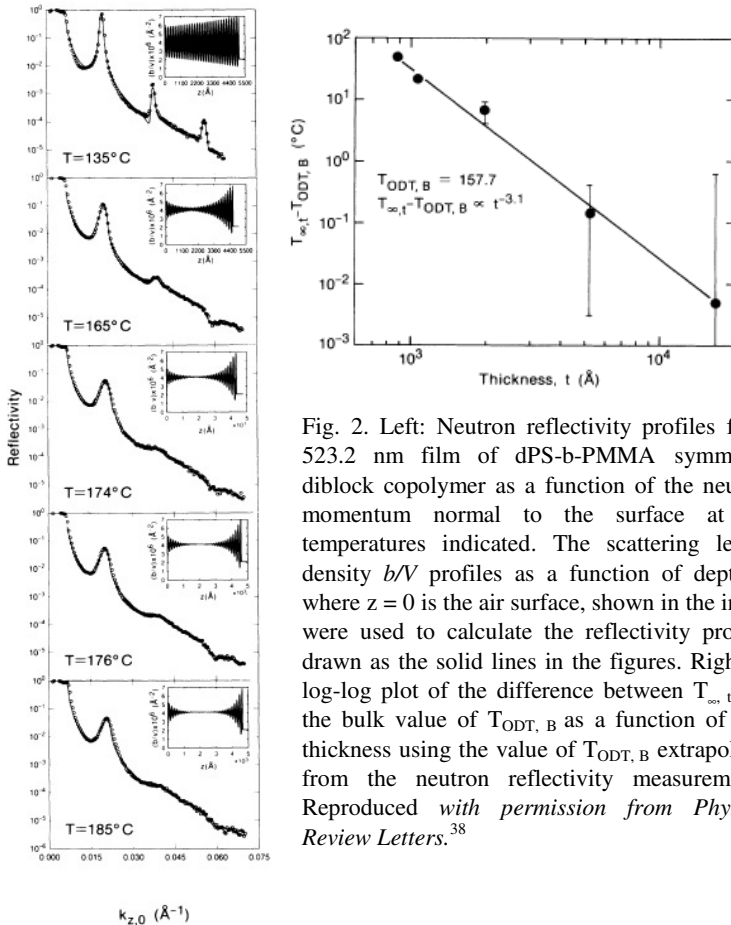


Fig. 2. Left: Neutron reflectivity profiles for a 523.2 nm film of dPS-*b*-PMMA symmetric diblock copolymer as a function of the neutron momentum normal to the surface at the temperatures indicated. The scattering length density b/V profiles as a function of depth z , where $z = 0$ is the air surface, shown in the insets were used to calculate the reflectivity profiles drawn as the solid lines in the figures. Right: A log-log plot of the difference between $T_{\infty,t}$ and the bulk value of $T_{\text{ODT},B}$ as a function of film thickness using the value of $T_{\text{ODT},B}$ extrapolated from the neutron reflectivity measurements. Reproduced with permission from *Physical Review Letters*.³⁸

the components to the interfaces. Any slight incommensurability will cause the microdomains to orient normal to the surface. The interfacial energies of an *A-b-B* BCP with a solid surface can be precisely controlled by anchoring a random copolymer of A and B, *A-r-B*, to the surface, where the volume fraction, f , of A monomers in the brush can be varied in the synthesis. As f is varied from 0 to 1, the system goes from a condition of preferential wetting of the substrate by A to a preferential wetting by B. However, for one specific value of f the interactions of A and B with the substrate are balanced. This was demonstrated with styrene and methyl methacrylate pairs and it was

found that a P(S-*r*-MMA) brush surface has equal interfacial energies with PS and PMMA when $f \cong 0.57$ (Figure 3).⁴³ The use of random

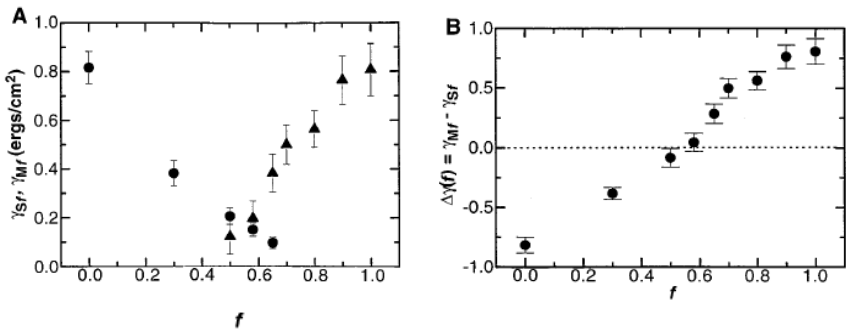


Fig. 3. (A) Interfacial energies γ_{Sf} and γ_{Mf} and (B) $\Delta\gamma(f) = \gamma_{Mf} - \gamma_{Sf}$ for PS (circles) and PMMA (triangles) on a P(S-*r*-MMA) brush as a function of f . Reproduced with permission from *Science*.⁴³

copolymers to modify and control interfacial interactions requires a simple synthetic method. Figure 4A shows the synthesis of (PS-*r*-MMA)

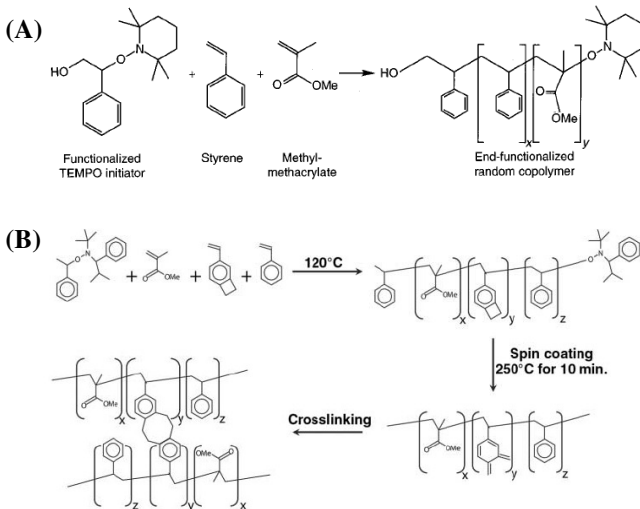


Fig. 4. (A) Schematic synthesis of P(S-*r*-MMA); (B) Schematic synthesis of P(S-*r*-BCB-*r*-MMA) which has 2% reactive benzocyclobutene (BCB) functionality randomly incorporated along the backbone that can be thermally crosslinked. Reproduced with permission from *Science*.^{43, 50}

random copolymers by a “living” free-radical polymerization using a unimolecular initiator which has a hydroxyl (OH) group that can be used to end-graft the random copolymer chains to the native silicon oxide surface.⁴³ However, this covalent attachment of the random copolymer to the surface requires substrate-specific chemistry which limits applications. Hawker and Russell et al.⁵⁰ modified the reaction and synthesized a random copolymer containing crosslinkable groups in the chain. Using a simple, highly efficient cross-linking reaction, an insoluble, ultrathin mat of the random copolymer can be formed which is more robust than anchored random copolymer brushes and is independent of the nature of the substrate (Figure 4B) and, as such, can be used to modify virtually any surface on which a thin film could be prepared.

Using anchored and crosslinked random copolymers, Russell and coworkers^{44, 46, 49, 52, 53, 56} quantitatively studied the influence of interfacial energies on the orientation of symmetric PS-*b*-PMMA microdomains in thin films. For BCP films placed on random copolymer brushes rich in PS, the PS block segregated to the random copolymer interface, leading to symmetric wetting. (The PS block segregates to the polymer/air interface due to its lower surface energy.) Conversely, PS-*b*-PMMA films on PMMA-rich random copolymers showed asymmetric wetting due to the wetting of the random copolymer layer with the PMMA block. For BCP films cast on random copolymer modified surfaces where interfacial interactions were balanced, preferential segregation of either block did not occur. This condition means that either A or B or both blocks could be located at the interface. Any film thickness that introduces a condition of incommensurability will result in an orientation of the microdomains normal to the interface. It should be noted that by balancing interfacial interactions, commensurability conditions are not the same as when there is a strong preference for either component to the interface. In fact, commensurability can be realized when the film thickness is $n/2L_0$, where n is an integer. This effectively means that an interface can cut a microdomain through the center, i.e. half cylinders or half lamellar layers located at the interface, and still satisfy the constraints imposed by the hard walls. Outside of this condition, if interfacial interactions are balanced, the microdomains are

oriented normal to the interface with the orientation persisting through the entire film thickness. Thus, by varying the composition of the random copolymer brushes, four boundary conditions can be achieved as shown in Figure 5.

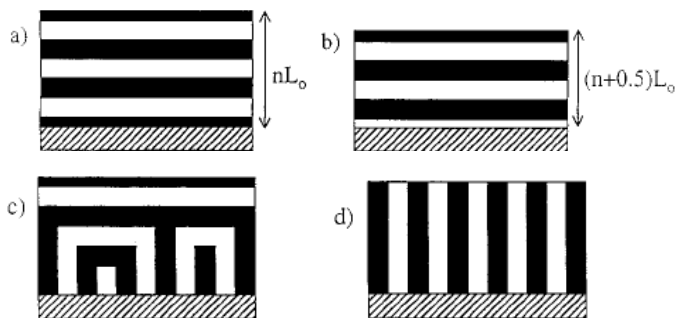


Fig. 5. Block copolymer structures observed for films having (a) symmetric boundary conditions, (b) asymmetric boundary conditions, (c) one nonpreferential and one preferential boundary surface, and (d) nonpreferential boundaries. Reproduced with permission from *Macromolecules*.⁴⁶

Modifying a solid substrate, as described above, can easily be achieved by anchoring a brush to the substrate or by placing a thin crosslinked film on the substrate. However, controlling interactions at the opposite interface, either the air surface or the second hard boundary placed in contact with the free surface, is not as straightforward. This can be achieved by transferring a random copolymer film on top of the BCP film, followed by placing the second hard wall in contact with this transferred layer. Alternatively, a polymer film where interactions between the blocks and this polymer are balanced can be spin-coated on top of the BCP film, as long as a non-solvent for the BCP is used.

2.3. Heterogeneous Surfaces

The strength and lateral distribution of interfacial interactions can direct the BCP morphologies in thin films.⁵⁷⁻⁶⁰ Surfaces where the interfacial interactions were laterally heterogeneous and periodic were used to

selectively place blocks at specific locations on a surface. Kramer and coworkers⁵⁷ experimentally demonstrated this by designing a surface where CH₃- and HO- terminated thiols were periodically modified on a gold surface to precisely tune the surface potential. This led to a preferential wetting of the components across the surface. Rockford et al.⁵⁸ investigated the ordering of BCP ultrathin films on chemically heterogeneous surfaces and found that highly ordered lamellar structures perpendicular to the surface could be obtained on a patterned surface with the period of the surface pattern within 10% of commensuration with the period of BCPs, L_0 . When the mismatch is greater than 10%, the lamellar microdomains orient parallel to the surface.⁵⁹ By using soft-x-ray-based photolithographic process to make chemically patterned substrates precisely, Nealey and coworkers⁶¹⁻⁶⁶ have significantly improved direct assembly of BCP thin films on chemically heterogeneous surfaces. Not only have they shown that the patterning can direct the morphology but that the copolymers can be used to improve the line-edge roughness of the features lithographically placed on the surface which is a technologically critical problem in nanolithography.

Heterogeneous surfaces with a gradient in length scales, from the nanoscopic to the microscopic, can also be produced by using mixtures of homopolymers and BCPs to act as templates for surface patterning.^{67, 68} In particular, by blade coating heterogeneous surfaces can be prepared, though such surfaces have not been used to control the orientation or ordering of BCPs.

3. Nanopatterning from BCP Thin Films

The self-assembly of BCPs into arrays of nanoscopic elements makes them ideal candidates as templates and scaffolds for the fabrication of nanostructured materials. While self-assembly generates the arrays of elements, it is necessary to harness the self-assembly so as to spatially direct the assembly into usable structures. This may simply mean controlling the orientation of the microdomains into arrays oriented parallel or normal to the surface of the film without any concern over the

lateral ordering of the microdomains. Indeed applications ranging from low dielectric constant insulators to filtration membranes for virus particles have already been realized using such a directed self-assembly concept where only the orientation of the microdomains is controlled. However, if BCP thin films are used as templates for addressable media or for polarization applications, it is necessary to control both the orientation and the ordering of the microdomains to a high degree and a biased, directed self-assembly must be used. Here, top-down approaches, like photolithography, which are used to pattern or sector a surface and are coupled with a bottom-up approach, like self-assembly, to obtain multi-length scales control over the ordering and spatial location of nanoscopic elements for device fabrication. Approaches to control the orientation of BCP microdomains include the use of solvent fields,⁶⁹⁻⁷³ electric fields,⁷⁴ chemically patterned substrates,^{62, 63} epitaxial crystallization,⁷⁵ graphoepitaxy,⁷⁶ controlled interfacial interactions,⁴³ thermal gradients,⁷⁷ zone casting,⁷⁸ optical alignment,^{79, 80} and shear.⁸¹⁻⁸³ This section will discuss long-range ordering of BCP thin films induced by solvent annealing, zone casting and optical alignment approaches that have been used effectively.

3.1. Solvent Annealing

The preparation of BCP thin films under various solvent evaporation conditions is an effective way to manipulate the orientation and lateral ordering of BCP microdomains in thin films. The solvent evaporation rate is one of the key factors that control these kinetically trapped nanostructures. For instance, inverted phases consisting of spheres or cylinders of the majority fraction block in a polystyrene-*block*-polybutadiene-*block*-polystyrene (PS-*b*-PB-*b*-PS) copolymer, which were not predicted on the basis of typical thermodynamic considerations for block copolymer melts, were observed by the control over the solvent evaporation rate.^{84, 85} Libera and coworkers first reported that solvent evaporation could be used to induce the ordering and orientation of BCP microdomains.^{69, 70, 86} Vertically aligned cylindrical PS microdomains could be obtained in a PS-*b*-PB-*b*-PS triblock copolymer thin films with

a thickness of ~ 100 nm.⁷⁰ The same effect was also observed in a polystyrene-*block*-poly(ethylene oxide) (PS-*b*-PEO) BCP thin films and was attributed to a copolymer/solvent concentration gradient along the direction normal to the film surface giving rise to an ordering front that propagated into the film during solvent evaporation.⁸⁷ This orientation was independent of the substrate. However, the lateral ordering of the cylindrical microdomains was poor. Sibener⁸⁸ and later Russell et al.⁷³ showed that evaporation-induced flow, in solvent cast BCP films, produced arrays of nanoscopic cylinders oriented normal to the surface with a high degree of ordering. Recently, Krausch and coworkers^{86, 89} demonstrated that solvent annealing could markedly enhance the ordering of BCP microdomains in thin films. By controlling the rate of solvent evaporation and solvent annealing in thin films of PS-*b*-PEO, Russell and coworkers^{71, 72} achieved nearly-defect-free arrays of cylindrical microdomains oriented normal to the film surface that spanned the entire films. Moreover, the use of a co-solvent enabled further control over the length scale of lateral ordering. Our most recent results⁹¹ showed that cylindrical microdomains oriented normal to the film surface could be obtained directly by spin-coating polystyrene-*block*-poly(4-vinylpyridine) (PS-*b*-P4VP) BCPs from mixed solvents of toluene and tetrahydrofuran (THF) (Figure 6(a)) and arrays of highly ordered cylindrical microdomains formed over large areas (Figure 6(b)) after exposing the films in the vapor of a toluene/THF mixture for a while. This process was independent of substrates, but strongly dependent on the quality of the solvents for each block and the solvent evaporation rate.

Solvent-induced surface reconstruction has been used to generate nanoporous templates from highly oriented PS-*b*-PMMA thin films.⁹⁰ By modifying the interfacial interactions with an anchored random copolymer, arrays of PMMA cylinders oriented normal to the film surface could be produced. By exposing the films to acetic acid, PMMA was solvated, while the glassy PS matrix remained intact. Upon drying, a film reconstruction was observed where pores were opened in the positions of the original PMMA cylinders as the PMMA within the pores was transferred to the surface. This pore generation is completely reversible such that, by heating the film above the glass transition

temperature of the PMMA, the original morphology was regenerated. A similar method was also used to generate nanoporous structures in PS-*b*-P4VP BCP thin films by using ethanol to draw the P4VP to the surface.⁹¹

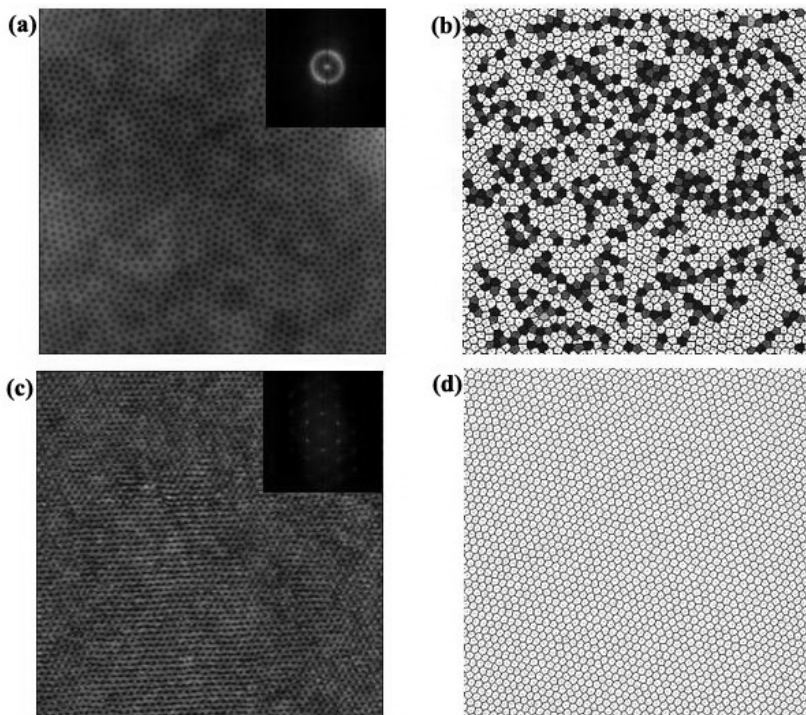


Fig. 6. A PS-*b*-P4VP thin film obtained by spin-coating ($2\ \mu\text{m} \times 2\ \mu\text{m}$): (a) SFM height images of an as-spun film; (c) SFM height images of a highly ordered and oriented array of cylindrical microdomains after solvent annealing. Insets are the corresponding Fourier transform spectra. (b, d) the corresponding Voronoi diagrams. Reproduced with permission from *ACS Nano*.⁹¹

3.2. Zone Casting

Zone-casting originally developed for the oriented growth of molecular crystals, has been used to achieve large-scale alignment of nanoscale domains in micro-phase separated BCPs.⁷⁹ Kowalewski and coworkers demonstrated a large-scale, long-range ordering of lamellae in thin films

of poly(*n*-butyl acrylate)-*block*-poly(acrylonitrile) (PBA-*b*-PAN) BCPs by using a simple zone-casting technique.⁷⁸ Zone-casting was performed by depositing the copolymer solution from *N, N*-dimethylformamide (DMF) onto a moving substrate with the aid of a syringe equipped with a flat nozzle. To achieve the desirable solvent evaporation rate, the temperatures of the copolymer solution and of the substrate were controlled. It should also be noted that, by varying the casting condition, the orientation of the microdomains with respect to the casting direction could be controlled.

3.3. Optical Alignment

Optical-alignment method on the molecular level is well-established in liquid-crystalline systems.^{92, 93} Directionally selective light excitation, using linearly polarized light of photoisomerizable molecules in a liquid-crystalline polymer produced patterned, oriented microdomains in the films. Recent investigations have revealed that such photoexcited collective molecular motions can lead to lateral mass transport over distances of micrometers.^{94, 95} Seki and coworkers⁹⁶ proposed an optical 3-D (both out-of-plane and in-plane) alignment of nanocylinders of a BCP comprised of a liquid-crystalline photo-responsive block and a PEO block by applying the concept of photo-induced mass migration. The key for out-of-plane alignment (whether the cylinders are oriented normal to or parallel to the substrate surface) is the control of the film thickness, while that for the in-plane alignment is the direction of polarization of the light during the illumination (Figure 7). Moreover, Ikeda and coworkers⁸⁰ demonstrated a noncontact-optical method by using polarized light to control a parallel patterning of PEO nanocylinders in an amphiphilic- liquid-crystalline BCP film.

3.4. Shearing

BCPs in bulk can easily be aligned by mechanical shear.^{81, 82} This technique has been widely used to align lamellar, cylindrical, spherical, and bicontinuous microdomains, but was limited to relatively thick films.

Recently, Register, Chaikin and coworkers^{81, 82} have demonstrated that a single layer of cylindrical microdomains⁸¹ and bilayers of spherical microdomains⁸² in BCP thin films can be aligned by applying shear. In their experiment, a PDMS pad is placed in contact with a heated BCP film. When subjected to a lateral motion, the stamp elastically distorts and shears the BCP thin film reorienting the microdomains in the direction of the applied shear.

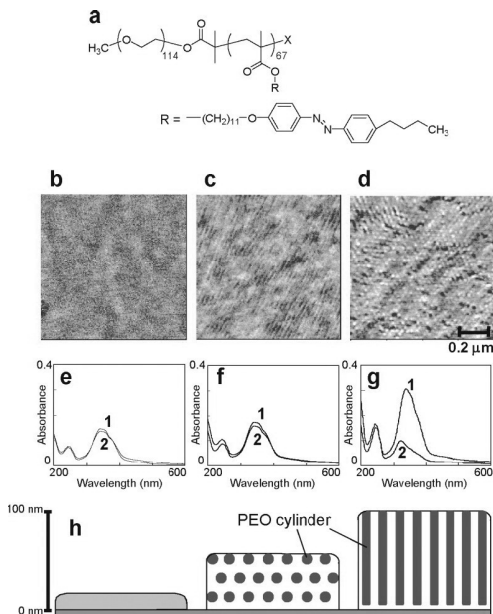


Fig. 7. Thickness dependence of the azobenzene (Az) and cylinder alignment. a) Chemical structure of the diblock copolymer consists of PEO and poly(methacrylate) containing an Az unit. b–d) Phase-mode AFM images ($1 \mu\text{m} \times 1 \mu\text{m}$) of the $p(\text{EO}_{114}\text{-Az}_{67})$ film with different film thickness: b) 20 nm, c) 30 nm, and d) 70 nm after annealing and exposure to hexane vapor. e–g) UV-vis absorption spectra of the corresponding $p(\text{EO}_{114}\text{-Az}_{67})$ films are shown: e) 20 nm, f) 30 nm, and g) 70 nm thickness for as-cast (1) films and after exposure to hexane vapor (2). h) Schematic illustration of thickness dependence on cylinder alignment. Reproduced with permission from *Advanced Materials*.⁹⁶

4. Applications of Nanopatterned BCP Thin Films

4.1. Nanoporous Membrane for Filtration of Viruses

Ultrafiltration membranes with small pore sizes have been used for the separation of viruses.^{97, 98} However, they were not very effective, since the virus particles permeates through a small number of abnormally large sized pores.⁹⁷ Track-etched polycarbonate (PC) and anodized aluminum oxide (AAO) membranes with uniform pore sizes have also been studied for the separation of viruses. While the pore size distributions are narrow

for these membranes, both types of membranes show a very low flux for virus separation.⁹⁸ Thus, a new type of membrane, providing both high selectivity and high flux, was needed for this purpose. Recently, Yang et al. introduced a new membrane with an asymmetric film geometry, which shows both high selectivity and high flux.⁹⁹ Figure 8 shows schematic diagram of the fabrication of asymmetric nanoporous membranes. This membrane consists of a thin nanoporous layer, prepared from a PS-*b*-PMMA BCP template (~ 80 nm thick film with cylindrical pores of ~ 15 nm in diameter and a narrow pore size distribution), and a supported membrane that provides mechanical strength. This asymmetric membrane showed ultrahigh selectivity while maintaining a high flux for the separation of human rhinovirus type 14 (HRV14), which has a diameter of ~ 30 nm.¹⁰³ This virus is a major pathogen for the common cold in humans. Since the pore diameter in the top layer can be tuned from 10 to 40 nm by changing the molecular weights of BCP or by adding a homopolymer miscible with the minor component of the BCP,^{100, 101} the cutoff size of the membrane filter could be precisely controlled.

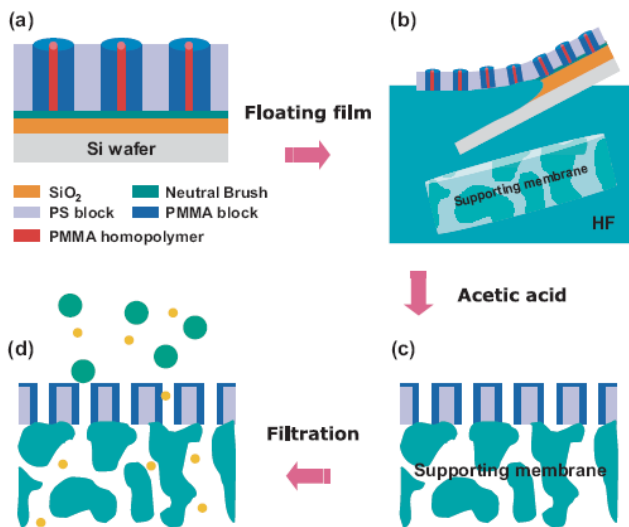


Fig. 8. Schematic depiction of the procedure for the fabrication of asymmetric nanoporous membranes. Reproduced with permission from *Advanced Materials*.⁹⁹

With these pore sizes, these asymmetric membranes allow biomolecules like proteins, present in the unfiltered solution, to pass through the membrane, while only the viruses are screened. The unique characteristic of this new membrane filter eliminates the risk of contamination from viruses while processing biotherapeutic proteins such as vaccines and hormones. Therefore, this new membrane can be used to develop new types of blood filtering systems, such as a haemodialysis membrane that is free of the risk of viral infection.

4.2. Incorporation of Nanocrystals and Nanoreactors

Quantum size effects and large surface to volume ratios contribute to the unusual properties of inorganic nanoparticles and studies of these effects have sparked great interests in novel fabrication processes of metal or metal oxide nanoparticles. The synthesis of nanoparticles from BCP microdomains is an effective route to control the size distributions, shapes, and spatial placements of nanoparticles. In the simplest rendition, one may use BCPs where one block has a higher affinity to the inorganics. For instance, Jaeger and coworkers demonstrated that metals deposited directly to the surface of a film would segregate into the underlying microdomains.¹⁰² The formation of ordered patterns is also possible by assembling BCP micelles upon casting, which has evoked a major interest for potential applications. Micellar cores offer a unique microenvironment, namely a nanoreactor, where inorganic precursors can be loaded and then processed by wet chemical methods to produce nanoparticles with a narrow size distribution, in a similar way as it is done with microemulsions.¹⁰³ The ordered deposition of gold and silver nanoclusters from micellar PS-*b*-P4VP^{104, 105} and PS-*b*-PAA¹⁰⁶ have been reported.

4.3. Planar Optical Waveguide

While polymer-based optical waveguide materials have been widely discussed,¹⁰⁷ little attention has been paid to BCP systems in regard to their applications in the field of optical elements. Kim et al.¹⁰⁸

demonstrated that thin films of BCPs with controlled orientation of microdomains can be used as planar optical waveguides and they investigated the waveguiding properties using optical waveguide spectroscopy (OWS).^{109, 110} Thin films of mixtures of PS-*b*-PMMA and PMMA homopolymers, with cylindrical PMMA microdomains oriented normal to the film plane, were used as optical waveguides with light being coupled into the film at different modes. The nanofabrication processes occurring inside the layer were monitored by OWS. The confinement of the PMMA homopolymer to the microdomains markedly enhances the aspect ratio of the microdomains by ~ 10 times over that seen in the bulk period,¹¹¹ which makes the film suitable for waveguiding applications. Resonance coupling between surface plasmons (or plasmon surface polaritons) and incident photons can occur at a metal/dielectric interface, especially in the experimental setup known as the Kretschmann configuration (Figure 9).^{109, 112} If the thickness of the dielectric layer is

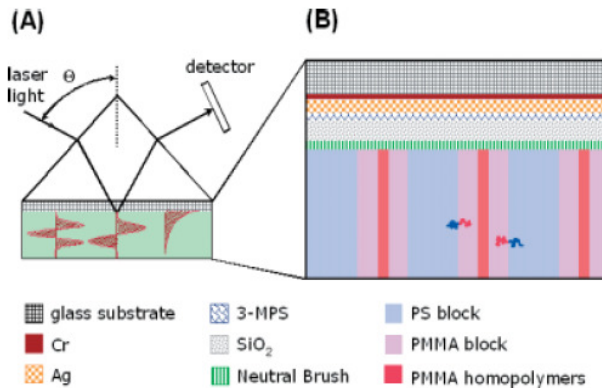


Fig. 9. A) Schematic diagram of the OWS setup based on the Kretschmann configuration, and of the idealized field distributions of several guided modes in the waveguiding layer. B) Schematic diagram of a thin film of PS-*b*-PMMA/PMMA homopolymer mixture with PMMA microdomains aligned normal to the substrate surface fabricated onto glass substrate. PS: polystyrene; PMMA: poly(methyl methacrylate); 3-MPS: 3-mercaptopropyl trimethoxysilane. Reproduced with permission from *Advanced Materials*.¹⁰⁸

further increased (in organic polymeric layers typically thicker than ~ 200 nm), waveguide optical modes, in addition to surface plasmon resonance, can be observed.^{109, 110}

4.4. *Templated Growth of Nanowires*

An advantage of the cylindrical microdomains in BCPs is the high aspect ratio and non-connectivity of the microdomains. For a 20- μm -thick film containing cylindrical microdomains that are 20 nm in diameter, an aspect ratio of 1000:1 is obtained. This advantage has been used where, under an applied electric field, the cylindrical microdomains of PMMA were oriented normal to the surface in films with thicknesses of ~ 30 μm . Thurn-Albrecht et al.⁷⁴ oriented the PMMA cylindrical microdomains in a PS-*b*-PMMA BCP by applying an electric field across the polymer film (Figure 10). Upon removal of the PMMA microdomains, metals, including cobalt, lead, and iron were placed

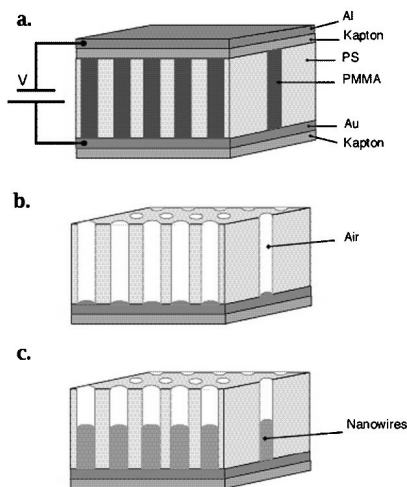


Fig. 10. Left: A schematic representation of high-density nanowire fabrication in a polymer matrix. (a) An asymmetric diblock copolymer annealed above the glass transition temperature of the copolymer between two electrodes under an applied electric field, forming a hexagonal array of cylinders oriented normal to the film surface. (b) After removal of the minor component, a nanoporous film is formed. (c) By electrodeposition, nanowires can be grown in the porous template, forming an array of nanowires in a polymer matrix. Reproduced with permission from *Science*.⁷⁴

within the nanopores by electrochemical deposition. The cobalt nanowires showed a single magnetic domain behavior⁷⁴ and enhanced coercivities¹¹³ in comparison to continuous cobalt films, and hold promise for use in ultrahigh-density magnetic storage devices (approaching one terabit per square inch). The effectiveness of nanoporous PS-*b*-PMMA thin films in generating such structures has motivated in-depth work in optimizing the fidelity of the structures and controlling the feature sizes.¹¹⁴

In addition to above mentioned applications, BCP thin films have received attention for use in the nanolithography process. The periodic nanostructure patterns of BCP films can be subsequently transferred to various kinds of substrates by a standard lithographic ion-etching process, due to the different etching sensitivities of the two building blocks. The regular nanopattern achieved can be used for a variety of applications, like high-density magnetic recording media, and quantum dot arrays.^{115,116} Another application of BCP thin films is in photonic materials. This is especially the case of BCP thin films that self-assemble into well-defined alternating layered structures.¹¹⁷

5. Summary and Outlook

Recent research efforts have demonstrated the utility of BCP thin films as components in a new generation of optical and electronic devices. Lithographic and micro-fabrication techniques using BCP thin films offer unprecedented feature dimensions and densities. Moreover, elegant methods of harnessing the microphase separation to produce ordered dispersions of inorganic nanoparticles are being developed. However, for many potential applications, e.g., addressable memory devices, limitations arise from imperfections in the long-range lateral order and the restricted choice of motifs. Significant advances have been made, though, by exploiting interfacial interactions and confinement effects, the use of external fields, and the use of chemically and topographically patterned substrates. Such morphological control, necessary in any applications, evolved directly from research on the fundamental physics, chemistry and engineering of BCP films. Further control in generating

hierarchical assemblies with 3-D structures can easily be envisioned with BCPs where control over structures and assembly on multiple length scales will be possible.

References

1. S. H. Anastasiadis, T. P. Russell, S. K. Satija, C. F. Majkrzak, *Physical Review Letters* 62, 1852 (1989).
2. S. H. Anastasiadis, T. P. Russell, S. K. Satija, C. F. Majkrzak, *The Journal of Chemical Physics* 92, 5677 (1990).
3. G. Coulon, T. P. Russell, V. R. Deline, P. F. Green, *Macromolecules* 22, 2581 (1989).
4. C. S. Henkee, L. T. Edwin, L. J. Fetters, *Journal of Materials Science* 23, 1685 (1988).
5. T. P. Russell, A. Menelle, S. H. Anastasiadis, S. K. Satija, C. F. Majkrzak, *Macromolecules* 24, 6263 (1991).
6. N. Koneripalli, N. Singh, R. Levicky, F. S. Bates, P. D. Gallagher, S. Satija, *Macromolecules* 28, 2897 (1995).
7. G. J. Kellogg, D. G. Walton, A. M. Mayes, P. Lambooy, T. P. Russell, P. D. Gallagher, S. K. Satija, *Physical Review Letters* 76, 2503 (1996).
8. A. M. Mayes, G. J. Kellogg, D. G. Walton, P. Lambooy, T. P. Russell, *Polymeric Materials Science and Engineering* 71, 282 (1994).
9. D. G. Walton, G. J. Kellogg, A. M. Mayes, P. Lambooy, T. P. Russell, *Macromolecules* 27, 6225 (1994).
10. P. Mansky, T. P. Russell, *Macromolecules* 28, 8092 (1995).
11. A. M. Mayes, S. K. Kumar, *MRS Bulletin* 22, 43 (1997).
12. T. P. Russell, A. M. Mayes, P. Bassereau, *Physica A: Statistical Mechanics and Its Applications* 200, 713 (1993).
13. T. P. Russell, P. Lambooy, G. J. Kellogg, A. M. Mayes, *Physica B: Condensed Matter* 213&214, 22 (1995).
14. T. P. Russell, P. Lambooy, G. J. Kellogg, A. M. Mayes, *Macromolecules* 28, 787 (1995).
15. A. M. Mayes, T. P. Russell, V. R. Deline, S. K. Satija, C. F. Majkrzak, *Macromolecules* 27, 7447 (1994).
16. A. M. Mayes, T. P. Russell, P. Bassereau, S. M. Baker, G. S. Smith, *Macromolecules* 27, 749 (1994).
17. M. J. Fasolka, A. M. Mayes, *Annual Review of Materials Research* 31, 323 (2001).
18. P. F. Green, R. Limary, *Advances in Colloid and Interface Science* 94, 53 (2001).
19. P. Lambooy, T. P. Russell, G. J. Kellogg, A. M. Mayers, P. D. Gallagher, S. K., Satija, *Physical Review Letters* 72, 2899 (1994).
20. P. Lambooy, J. R. Salem, T. P. Russell, *Thin Solid Films* 252, 75 (1994).
21. M. Kikuchi, K. Binder, *Europhysics Letters* 21, 427 (1993).
22. M. Kikuchi, K. Binder, *The Journal of Chemical Physics* 101, 3367 (1994).
23. M. S. Turner, *Physical Review Letters* 69, 1788 (1992).
24. P. F. Green, T. M. Christensen, T. P. Russell, R. Jerome, *The Journal of Chemical Physics* 92, 1478 (1990).

25. R. Limary, P. F. Green, *Macromolecules* 32, 8167 (1999).
26. P. F. Green, T. M. Christensen, T. P. Russell, *Macromolecules* 24, 252 (1991).
27. P. F. Green, T. M. Christensen, T. P. Russell, R. Jerome, *Macromolecules* 22, 2189 (1989).
28. F. Brochard-Wyart, P. Martin, C. Redon, *Langmuir* 9, 3682 (1993).
29. A. R. Segalman, P. F. Green, *Macromolecules*, 801 (1990).
30. J. L. Masson, P. F. Green, *The Journal of Chemical Physics* 112, 349 (2000).
31. G. Brown, A. Chakrabarti, *The Journal of Chemical Physics* 101, 3310 (1994).
32. Y. Liu, W. Zhao, X. Zheng, A. King, A. Singh, M. H. Rafailovich, J. Sokolov, K. H. Dai, E. J. Kramer, *Macromolecules* 27, 4000 (1994).
33. K. R. Shull, E. J. Kramer, F. S. Bates, J. H. Rosedale, *Macromolecules* 24, 1383 (1991).
34. T. P. Russell, A. Menelle, S. H. Anastasiadis, S. K. Satija, C. F. Majkrzak, *Progress in Colloid & Polymer Science* 91, 97 (1993).
35. B. J. Factor, T. P. Russell, M. F. Toney, *Physical Review Letters* 66, 1181 (1991).
36. T. P. Russell, G. Coulon, V. R. Deline, D. C. Miller, *Macromolecules* 22, 4600 (1989).
37. T. P. Russell, A. Menelle, S. H. Anastasiadis, S. K. Satija, C. F. Majkrzak, *Makromolekulare Chemie, Macromolecular Symposia* 62, 157 (1992).
38. A. Menelle, T. P. Russell, S. H. Anastasiadis, S. K. Satija, C. F. Majkrzak, *Physical Review Letters* 68, 67 (1992).
39. C. S. Henkee, E. L. Thomas, L. J. Fetters, *Journal of Materials Science* 23, 1685 (1988).
40. L. T. J. Korley, B. D. Pate, E. L. Thomas, P. T. Hammond, *Polymer* 47, 3073 (2006).
41. E. L. Thomas, E. J. Roche, *Polymer* 20, 1413 (1979).
42. H. Fredrickson Glenn, *Macromolecules* 20, 2535 (1987).
43. P. Mansky, Y. Liu, E. Huang, T. P. Russell, C. Hawker, *Science* 275, 1458 (1997).
44. E. Huang, P. Mansky, T. P. Russell, C. Harrison, P. M. Chaikin, R. A. Register, C. J. Hawker, J. Mays, *Macromolecules* 33, 80 (2000).
45. M. Husseman, E. E. Malmstroem, M. McNamara, M. Mate, D. Mecerreyes, D. G. Benoit, J. L. Hedrick, P. Mansky, E. Huang, T. P. Russell, C. J. Hawker, *Macromolecules* 32, 1424 (1999).
46. E. Huang, S. Pruzinsky, T. P. Russell, J. Mays, C. J. Hawker, *Macromolecules* 32, 5299 (1999).
47. T. P. Russell, T. Thurn-Albrecht, M. Tuominen, E. Huang, C. J. Hawker, *Macromolecular Symposia* 159, 77 (2000).
48. Z. H. Cai, K. Huang, P. A. Montano, T. P. Russell, J. M. Bai, G. W. Zajac, *The Journal of Chemical Physics* 98, 2376 (1993).
49. E. Huang, T. P. Russell, C. Harrison, P. M. Chaikin, R. A. Register, C. J. Hawker, J. Mays, *Macromolecules* 31, 7641 (1998).
50. D. Y. Ryu, K. Shin, E. Drockenmuller, C. J. Hawker, T. P. Russell, *Science* 308, 236 (2005).
51. C. J. Hawker, T. P. Russell, *MRS Bulletin* 30, 952 (2005).
52. T. Xu, C. J. Hawker, T. P. Russell, *Macromolecules* 38, 2802 (2005).
53. P. Mansky, T. P. Russell, C. J. Hawker, M. Pitsikalis, J. Mays, *Macromolecules* 30, 6810 (1997).

54. C. J. Hawker, E. Elce, J. Dao, W. Volksen, T. P. Russell, G. G. Barclay, *Macromolecules* 29, 2686 (1996).
55. P. Mansky, T. P. Russell, C. J. Hawker, J. Mays, D. C. Cook, S. K. Satija, *Physical Review Letters* 79, 237 (1997).
56. P. Mansky, O. K. C. Tsui, T. P. Russell, Y. Gallot, *Macromolecules* 32, 4832 (1999).
57. J. Heier, Kramer E. J., S. Walheim, Krausch G., *Macromolecules*, 6610 (1997).
58. L. Rockford, Y. Liu, P. Mansky, T. P. Russell, M. Yoon, S. G. J. Mochrie, *Physical Review Letters* 82, 2602 (1999).
59. L. Rockford, S. G. J. Mochrie, T. P. Russell, *Macromolecules* 34, 1487 (2001).
60. M. Böltau, S. Walheim, J. Mlynek, G. Krausch, U. Steiner, *Nature* 391, 877 (1998).
61. S. Xiao, X. Yang, E. Edwards, Y.-H. La, P. F. Nealey, *Nanotechnology* 16, S324 (2005).
62. S. O. Kim, H. H. Solak, M. P. Stoykovich, N. J. Ferrier, J. J. de Pablo, P. F. Nealey, *Nature* 424, 411 (2003).
63. M. P. Stoykovich, M. Mueller, S. O. Kim, H. H. Solak, E. W. Edwards, J. J. de Pablo, P. F. Nealey, *Science* 308, 1442 (2005).
64. E. W. Edwards, M. F. Montague, H. H. Solak, C. J. Hawker, P. F. Nealey, *Advanced Materials* 16, 1315 (2004).
65. S.-M. Park, M. P. Stoykovich, R. Ruiz, Y. Zhang, C. T. Black, P. F. Nealey, *Advanced Materials* 19, 607 (2007).
66. M. P. Stoykovich, E. W. Edwards, H. H. Solak, P. F. Nealey, *Physical Review Letters* 97, 147802/1 (2006).
67. I. Y. Tsai, M. Kimura, T. P. Russell, *Langmuir* 20, 5952 (2004).
68. I. Y. Tsai, J. A. Green, M. Kimura, B. Jacobson, T. P. Russell, *Journal of Biomedical Materials Research part A*, 509 (2006).
69. G. Kim, M. Libera, *Macromolecules* 31, 2670 (1998).
70. G. Kim, M. Libera, *Macromolecules* 31, 2569 (1998).
71. S. H. Kim, M. J. Misner, T. P. Russell, *Advanced Materials* 16, 2119 (2004).
72. S. H. Kim, M. J. Misner, T. Xu, M. Kimura, T. P. Russell, *Advanced Materials* 16, 226 (2004).
73. M. Kimura, M. J. Misner, T. Xu, S. H. Kim, T. P. Russell, *Langmuir* 19, 9910 (2003).
74. T. Thurn-Albrecht, J. Schotter, G. A. Kastle, N. Emley, T. Shibauchi, L. Krusin-Elbaum, K. Guarini, C. T. Black, M. T. Tuominen, T. P. Russell, *Science* 290, 2126 (2000).
75. J. Y. Cheng, A. M. Mayes, C. A. Ross, *Nature Materials* 3, 823 (2004).
76. R. A. Segalman, H. Yokoyama, E. J. Kramer, *Advanced Materials* 13, 1152 (2001).
77. J. Bodycomb, Y. Funaki, K. Kimishima, T. Hashimoto, *Macromolecules* 32, 2075 (1999).
78. C. Tang, A. Tracz, M. Kruk, R. Zhang, D.-M. Smilgies, K. Matyjaszewski, T. Kowalewski, *Journal of the American Chemical Society* 127, 6918 (2005).
79. A. Tracz, J. K. Jeszka, M. D. Watson, W. Pisula, K. Muellen, T. Pakula, *Journal of the American Chemical Society* 125, 1682 (2003).
80. H. Yu, T. Iyoda, T. Ikeda, *Journal of the American Chemical Society* 128, 11010 (2006).
81. D. E. Angelescu, J. H. Waller, D. H. Adamson, P. Deshpande, S. Y. Chou, R. A. Register, P. M. Chaikin, *Advanced Materials* 16, 1736 (2004).

82. D. E. Angelescu, J. H. Waller, R. A. Register, P. M. Chaikin, *Advanced Materials* 17, 1878 (2005).
83. M. A. Villar, D. R. Rueda, F. Ania, E. L. Thomas, *Polymer* 43, 5139 (2002).
84. Q. Zhang, O. K. C. Tsui, B. Du, F. Zhang, T. Tang, T. He, *Macromolecules*, 33, 9561 (2000).
85. H. Huang, F. Zhang, Z. Hu, B. Du, T. He, *Macromolecules*, 36, 4084 (2003).
86. K. Fukunaga, H. Elbs, R. Magerle, G. Krausch, *Macromolecules* 33, 947 (2000).
87. Z. Q. Lin, D. H. Kim, X. D. Wu, L. Boosahda, D. Stone, L. LaRose, T. P. Russell, *Advanced Materials* 14, 1373 (2002).
88. J. Hahn, S. J. Sibener, *Langmuir* 16 4766 (2000).
89. K. Fukunaga, T. Hashimoto, H. Elbs, G. Krausch, *Macromolecules* 35, 4406 (2002).
90. T. Xu, J. Stevens, J. A. Villa, J. T. Goldbach, K. W. Guarini, C. T. Black, C. J. Hawker, T. P. Russell, *Advanced Functional Materials* 13, 698 (2003).
91. S. Park, J.-Y. Wang, B. Kim, J. Xu and T. P. Russell, *ACS Nano* 2, 766 (2008).
92. K. Ichimura, *Chemical Reviews* 100, 1847 (2000).
93. T. Ikeda, *Journal of Materials Chemistry* 13, 2037 (2003).
94. R. H. Berg, S. Hvilsted, P. S. Ramanujam, *Nature* 383, 505 (1996).
95. A. Natansohn, P. Rochon, *Chemical Reviews* 102, 4139 (2002).
96. Y. Morikawa, S. Nagano, K. Watanabe, K. Kamata, T. Iyoda, T. Seki, *Advanced Materials* 18, 883 (2006).
97. T. Urase, K. Yamamoto, S. Ohgaki, *Water Science and Technology* 30, 199 (1994).
98. T. Urase, K. Yamamoto, S. Ohgaki, *Journal of Membrane Science* 115, 21 (1996).
99. S. Y. Yang, I. Ryu, H. Y. Kim, J. K. Kim, S. K. Jang, T. P. Russell, *Advanced Materials* 18, 709 (2006).
100. U. Jeong, D. Y. Ryu, D. H. Kho, D. H. Lee, J. K. Kim, T. P. Russell, *Macromolecules* 36, 3626 (2003).
101. U. Jeong, D. Y. Ryu, J. K. Kim, D. H. Kim, T. P. Russell, C. J. Hawker, *Advanced Materials* 15, 1247 (2003).
102. W. A. Lopes, H. M. Jaeger, *Nature* 414, 735 (2001).
103. M. Breulmann, S. Forster, M. Antonietti, *Macromolecular Chemistry and Physics* 201, 204 (2000).
104. J. P. Spatz, S. Mössmer, C. Hartmann, M. Möller, T. Herzog, M. Krieger, H.-G. Boyen, P. Ziemann, B. Kabius, *Langmuir* 16, 407 (2000).
105. S.-H. Yun, S. I. Yoo, J. C. Jung, W.-C. Zin, B.-H. Sohn, *Chemistry of Materials* 18, 5646 (2006).
106. Y. Boontongkong, R. E. Cohen, *Macromolecules* 35, 3647 (2002).
107. H. Ma, A. K. Y. Jen, L. R. Dalton, *Advanced Materials* 14, 1339 (2002).
108. D. H. Kim, K. H. A. Lau, J. W. F. Robertson, O.-J. Lee, U. Jeong, J. I. Lee, C. J. Hawker, Russell, T. P. J. K. Kim, W. Knoll, *Advanced Materials* 17, 2442 (2005).
109. W. Knoll, *Annual Review of Physical Chemistry* 49, 569 (1998).
110. J. D. Swalen, *The Journal of Physical Chemistry* 83, 1438 (1979).
111. U. Jeong, D. Y. Ryu, D. H. Kho, J. K. Kim, J. T. Goldbach, D. H. Kim, T. P. Russell, *Advanced Materials* 16, 533 (2004).
112. E. Kretschmann, T. L. Ferrell, J. C. Ashley, *Physical Review Letters* 42, 1312 (1979).
113. T. Shibauchi, L. Krusin-Elbaum, L. Gignac, C. T. Black, T. Thurn-Albrecht, T. P. Russell, J. Schotter, G. A. Kastle, N. Emley, M. T. Tuominen, *Journal of Magnetism and Magnetic Materials* 226-230, 1553 (2001).

114. T. Xu, H.-C. Kim, J. DeRouchey, C. Seney, C. Levesque, P. Martin, C. M. Stafford, T. P. Russell, *Polymer* 42, 9091 (2001).
115. C. T. Black, R. Ruiz, G. Breyta, J. Y. Cheng, M. E. Colburn, K. W. Guarini, H.-C. Kim, Y. Zhang, *IBM Journal of Research & Development* 51, 606 (2007)
116. M. Park, C. Harrison, P. M. Chaikin, R. A. Register, D. H. Adamson, *Science* 276, 1401, *Science* 276, 1401 (1997).
117. Y. Fink, J. N. Winn, S. Fan, C. Chen, M. J. J. Jurgen, J. D. Joannopoulos, E. L. Thomas, *Science* 282, 1679 (1998).